Journal of Alloys and Compounds, *188* (1992) 179–181
JALCOM 9021

Iron–alumina interface in ceramic matrix nanocomposites

X. Devaux, Ch. Laurent, M. Brieu and A. Rousset
Laboratoire de Chimie des Matériaux Inorganiques, URA CNRS 1311, Université Paul-Sabatier, 31062 Toulouse Cedex (France)

Abstract

The composite powders investigated in the present study consisted of nanometric iron particles dispersed in an alumina matrix. According to the temperature of formation, iron particles are either directly epitaxied in the alumina matrix or separated from the alumina by a thin layer of iron aluminate spinel. This layer disappears after annealing under hydrogen. Transmission electron micrographic and electron microdiffraction pattern analyses led to a general epitaxial relationship between iron nanoparticles and alumina, which holds whatever the elaboration process. A mechanism for the crystallographical reorientation of the iron particles, when the spinel phase is reduced, is proposed.

1. Introduction

In previous works [1, 2] we investigated the toughening of alumina with nanometric iron particles. Since the enhancement of the mechanical properties of composite materials is partly related to the bonding characteristics at the interface, study of the alumina–iron interface is an important step in the understanding of toughening mechanisms.

In alumina–metal composites, the metal is either separated from the alumina matrix by a double oxide phase or is directly in contact with the alumina. Systems Al_2O_3–MAl_2O_4–M, where M stands for metal, are likely to exist when the MO oxide is easy to form and is then able to react with alumina to form an MAl_2O_4 spinel phase. For example, such systems were observed with M ≡ Cu, Ni, Fe by Wlosinski [3], Elssner and Petzow [4], and Ogale *et al.* [5] respectively. Direct epitaxy between Al_2O_3 and niobium, tungsten and platinum was observed by Qadri *et al.* [6], Souk *et al.* [7], and Mulder and Klomp [8] respectively, and also between Al_2O_3 and copper and iron by Wlosinski [3], and Anton *et al.* [9] respectively. The process of elaboration of the composite and the nature or shape of both the alumina (monocrystalline or polycrystalline) and metal (thin film, particles) are of great importance with respect to interfacial problems.

The composites studied here consisted of nanometric iron particles dispersed within micrometer sized alumina grains.

2. Experimental details

An alumina–hematite solid solution was prepared by a chemical process [10]. Nanocomposite powders were obtained by reduction of this solid solution under hydrogen at either "low" ($T < 800\,^{\circ}C$) or "high" ($T > 1000\,^{\circ}C$) temperatures for 10 h. The alumina-to-hematite ratio was such that a total conversion of hematite to metallic iron during the reduction process gave an alumina-to-iron mass ratio of 90/10.

X-ray diffraction (XRD), transmission electron microscopy (TEM) and electron microdiffraction (EMD) were performed on the powders. The specimens were prepared for TEM examinations by ultrasonic dispersion in ethanol. High resolution electron microscopy (HREM) was also performed on the powder reduced at high temperatures.

3. Results and discussion

3.1. High temperature reduction process

XRD pattern analysis reveals the presence of two phases only: α-Al_2O_3 and α-Fe. TEM observations show that most of the metal particles are dispersed within the alumina grains. The average size of the iron particles, evaluated by direct measurement of 1000 particles on TEM micrographs, is 10 nm (Fig. 1(a)).

Comparison between bright field and dark field micrographs, together with EMD pattern analysis (Fig. 1), shows that both the alumina grains and metal particles are monocrystalline, and that the intragranular iron particles have the same crystallographic orientation. EMD pattern indexation (Fig. 1(d)) leads to the following general epitaxial relationship:

$$(111)[\bar{1}\bar{1}2]_{\alpha\text{-Fe}}//(0001)[10\bar{1}0)_{\alpha\text{-}Al_2O_3}$$

Investigations of several EMD patterns of the same grain observed along various crystallographic orientations confirms this relationship. A similar relationship

0925-8388/92/$5.00

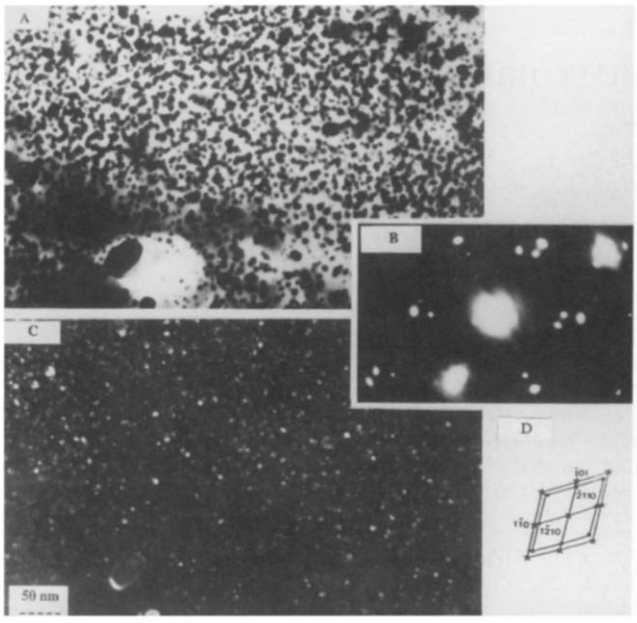

Fig. 1. TEM images of an alumina–iron nanocomposite reduced at high temperature: (a) bright field; (b) dark field; (c) EMD pattern; (d) EMD pattern indexation.

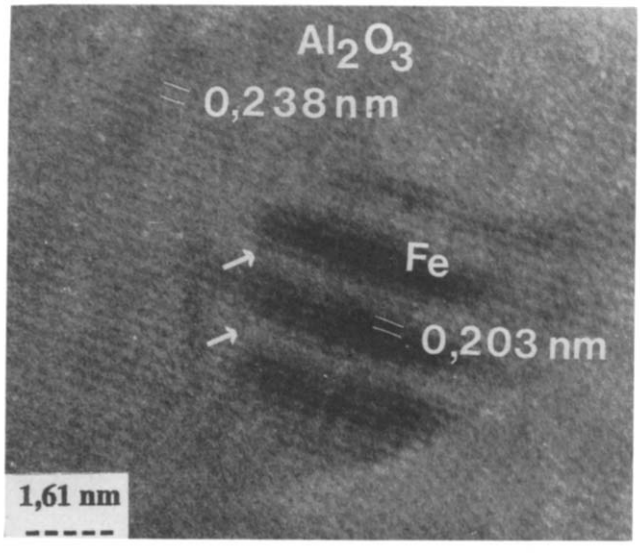

Fig. 2. HREM image of an alumina–iron nanocomposite reduced at high temperature. Arrows indicate dislocations at the interface.

was observed on thin films of b.c.c. metal (niobium [6], iron [9]) epitaxied on sapphire. An HREM image (Fig. 2) shows iron ($\bar{1}01$) planes parallel to alumina ($\bar{2}110$) planes. Dislocations, indicated by arrows on Fig. 2, are present at the interface to accommodate the lattice parameter mismatch. The darker stripes on the picture are Moiré fringes.

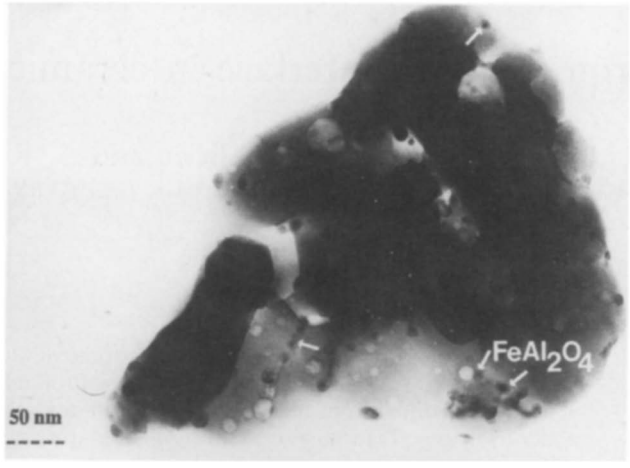

Fig. 3. TEM image of an alumina–iron nanocomposite reduced at low temperature.

3.2. Low temperature reduction process

As in the preceding specimen, only α-Al_2O_3 and α-Fe are detected by XRD. However, TEM observations reveal that some iron particles are surrounded by an interfacial phase (Fig. 3). This phase, 2–5 nm thick, was identified in previous work [11] using magnetic measurements as iron aluminate ($FeAl_2O_4$). This is consistent with observations of iron–alumina interfaces by Ogale *et al.* [5], and with the work of Imlach and Glasser [12] on phase equilibria in the system Fe–Fe_2O_3–Al_2O_3.

The metal particles do not have a common crystallographic orientation, depending on the presence of the iron aluminate layer. The composite powder was annealed under hydrogen at 800 °C for 50 h in order to reduce the $FeAl_2O_4$ and to determine whether the epitaxy of iron particles in the alumina matrix is a result of the γ-Fe $\longrightarrow$ α-Fe transformation which occurs at 910 °C during cooling down of the powder from the high temperature.

TEM observations of the annealed powder show that there is no longer an interfacial phase. The EMD patterns are similar to those obtained with the powder reduced at high temperature; thus there is epitaxy of α-Fe on alumina as soon as the interfacial layer disappears, and it seems likely that the crystallographic orientation of the iron particles which were not surrounded by the layer of iron aluminate was the same before the annealing treatment.

Works of Swann and Tighe [13] on the reduction of hematite to magnetite and of Pennock and Flower [14] on the reduction of magnetite to iron allow us to suppose that there are also epitaxial relationships between iron aluminate and alumina on the one hand, and between iron aluminate and iron on the other

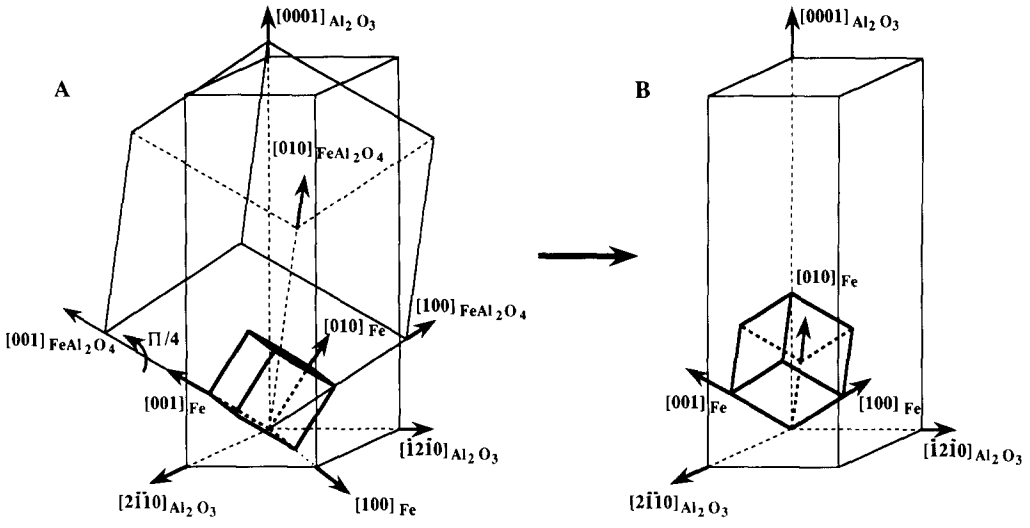

Fig. 4. Proposition for a mechanism of crystallographic reorientation of the iron particles during annealing under hydrogen in specimens reduced at low temperature: (a) before annealing; (b) after annealing.

hand. The following relationships are from refs. 13 and 14 respectively:

$(111)[0\bar{1}1]_{Fe_3O_4}//(0001)[10\bar{1}0]_{\alpha\text{-}Fe_2O_3}$

$(001)[110]_{\alpha\text{-}Fe}//(001)[100]_{Fe_2O_4}$

As the $Fe-FeAl_2O_4-Al_2O_3$ and $Fe-Fe_3O_4-Fe_2O_3$ systems are structurally equivalent, we assume the following epitaxial relationships in our system:

$(111)[0\bar{1}1]_{FeAl_2O_4}//(0001)[10\bar{1}0]_{\alpha\text{-}Al_2O_3}$

$(001)[110]_{\alpha\text{-}Fe}//(001)[100]_{FeAl_2O_4}$

These relationships are represented in Fig. 1(a) and the observed relationship, in the annealed powder, in Fig. 1(b). The mechanism for the crystallographic reorientation of the iron particles during annealing under hydrogen, when the spinel phase is reduced, can therefore be described by a $(\pi/4)$ rotation around the $[001]_{\alpha\text{-}Fe}$ axis (see curved arrow in Fig. 4).

4. Conclusions

At temperatures beyond 1000 °C, the reduction under hydrogen of an alumina–hematite solid solution leads to the formation of an alumina–iron nanocomposite, in which the iron nanoparticles are directly epitaxied on the alumina matrix. In composites elaborated using the same process but at temperatures below 800 °C, some iron particles are surrounded by an iron aluminate layer. The epitaxial relationship observed between the iron nanoparticles and the alumina matrix is obtained with α-Fe particles as soon as the interfacial phase disappears during the reduction process. Assuming that there is also epitaxy between iron and $FeAl_2O_4$, and between $FeAl_2O_4$ and Al_2O_3, a simple mechanism could describe the crystallographical reorientation of the iron particles.

References

1 A. Rousset, X. Devaux, M. Brieu and A. Marchand, *Proc. 10th Tsukuba General Symp., Tsukuba, Japan, October 2–3, 1990*, p. 134.
2 X. Devaux, Ch. Laurent, M. Brieu and A. Rousset, in A. T. DiBenetdetto, L. Nicolais and R. Watanabe (eds.), *Composite Materials, Strasbourg, France, May 1991*, Amsterdam, 1992, p. 209. *Proc. Int. Conf. on Advanced Materials, Symp. A4.*
3 W. K. Wlosinski, in G. S. Upadhyaya (ed.), *Sintered Metal–Ceramic composites*, Elsevier, Amsterdam, 1984, p. 483.
4 G. Elssner and G. Petzow, *Z. Metallkde., 64* (1973) 280.
5 S. B. Ogale, D. M. Phase, S. M. Chaudhari, S. V. Ghaisas, S. M. Kanetkar, P. P. Patil, V. G. Bhide and S. K. Date, *Phys. Rev. B, 35* (1987) 1593.
6 S. B. Qadri, J. H. Claassen, P. R. Broussard and S. A. Wolf, *J. Less-Common Met., 115* (1989) 327.
7 J. H. Souk, A. Segmuller and J. Angilello, *J. Appl. Phys., 62* (1985) 509.
8 C. A. M. Mulder and J. T. Klomp, *J. Phys. (Paris), 46* (1985) C4-111.
9 R. Anton, K. Heinemann and H. Poppa, *Vide Couches Minces, 201* (1980) 121.
10 A. Rousset and X. Devaux, *French Patent, 90 09790*, July 24, 1990.
11 X. Devaux, *French Thesis*, Toulouse, 1991, p. 166.
12 J. A. Imlach and F. P. Glasser, *Trans. J. Br. Ceram. Soc., 70* (1971) 227.
13 P. R. Swann and N. J. Tighe, *Metall. Trans. B, 8* (1977) 479.
14 G. M. Pennock and H. M. Flower, *Inst. Phys. Conf. Ser. 68, 8* (1983) 263.